Journal of the Indian Chemical Society 99 (2022) 100275

Contents lists available at ScienceDirect

Journal of the Indian Chemical Society

journal homepage: www.editorialmanager.com/JINCS/default.aspx

Flavonolignan silibinin abrogates SDS induced fibrillation of human serum albumin

Aalok Basu [a,b,*], Shovonlal Bhowmick [b], Arup Mukherjee [c]

[a] Dr. B.C. Roy College of Pharmacy and Allied Health Sciences, Bidhannagar, Durgapur, 713206, West Bengal, India
[b] Department of Chemical Technology, University of Calcutta, 92 A.P.C. Road, Kolkata, 700009, West Bengal, India
[c] Department of Biotechnology, Maulana Abul Kalam Azad University of Technology, BF 142, Sector 1, Salt Lake City, Kolkata, 700064, West Bengal, India

ARTICLE INFO

Keywords:
Silibinin
Protein fibrillation
Thioflavin T
Human serum albumin

ABSTRACT

Misfolding, aggregation and fibrillation of amyloidogenic proteins have been established as hallmark events in pathophysiology of various degenerative diseases. Inhibition of protein fibrillation through use of plant derived molecular scaffolds is currently considered as one solution to it. Further, rational design of therapeutic originating with the specific plant molecular scaffolds appeared passable to aid in mitigating amyloidogenic diseases. Silibinin (SB) is a flavonolignan obtained from milk thistle plant. SB is well acclaimed as a potent hepatoprotective, cardioprotective and an attenuator of receptor signaling in case of type 2 diabetes. This work reports the inhibitory capacity of SB against protein fibrillation under experimental conditions. Human serum albumin (HSA), an ubiquitous serum protein was used and various platform studies were carried out for indepth understanding of similar effects. Biophysical studies and electron microscopy confirmed that SB inhibited HSA fibrils formations by 36% at optimal molar ratio. *In silico* studies further demonstrated that intermolecular hydrogen bonds and hydrophobic interactions hindered progressive aggregation and protein fibrillation.

1. Introduction

Proteins perform several biological functions with high specificity, ascribed to their native three-dimensional structures [1,2]. Loss of conformational stability of proteins may lead to misfolding of their native structures and generation of highly ordered amyloid fibrils or amorphous aggregates [3]. The formed fibrils are typically stabilized through several inter- and intra-molecular interactions, and hence are resistant to thermal and chemical denaturation [4,5]. Till now, around thirty seven physiological proteins have been known to form amyloid deposits in tissues, and each of these forms has certain distinctive molecular features and different degrees of toxicity [6,7]. Deposition of fibrils and related insoluble oligomers in extracellular as well as intercellular spaces is the molecular hallmark of several degenerative conditions including Parkinson's disease, Alzheimer's disease and type 2 diabetes [8]. The possible strategies for prevention and mitigation of these diseases involve inhibition of the fibrillation process and clearance of amyloid aggregates from cellular matrices [9]. A number of studies can be found in literature which highlight the inhibition of amyloid fibrillation using small molecules, peptides, proteins, carbohydrates, nanoparticles and quantum dots [6,9]. However, there is no approved therapeutic available for the mitigation of amyloid related conditions [10].

Compounds from natural sources hold a pivotal place due to their structural diversity, minimum toxicity and druggability, and have been reported to deter amyloid fibrillation as well as disintegrate pre-existing fibrils [11]. Silibinin (or silybin) is a bioactive flavonolignan and constitutes 34% of silymarin, which is a flavonoid mixture obtained from the flowers and leaves of milk thistle (*Silybum marianum*) plant. The milk thistle plant has been used by different civilizations as a natural remedy for centuries, especially in amatoxin mushroom (*Amanita phalloides*) poisoning [12,13]. Renewed scientific interests in plant derived micronutrients in the past decade led to a number of publications related to silymarin [14]. The standardized mixture of silymarin containing silibinin, isosilybin, silychristin, silydianin and others, is now an essential part of contemporary medicines available for alleviation of several disease conditions [15–17]. Among the different components of silymarin, silibinin (SB) has attracted considerable research interests owing to its potent anti-oxidant [18], anti-inflammatory [19], anti-diabetic [20], as well as neuroprotective properties [21]. SB has also been investigated as an inhibitor of fibrillation of tissue specific proteins such as amyloid β, human islet amyloid polypeptide and insulin [22–24]. However, the fibrillation inhibitory mechanisms were different in each case and

* Corresponding author. Dr. B.C. Roy College of Pharmacy and Allied Health Sciences, Bidhannagar, Durgapur, 713206, West Bengal, India.
E-mail address: aalok.albus@gmail.com (A. Basu).

https://doi.org/10.1016/j.jics.2021.100275
Received 6 August 2021; Received in revised form 22 October 2021; Accepted 17 November 2021

pertained to the target polypeptide [25]. Studies on amyloid deposition using high resolution electron tomography revealed that fibril network formations under *in vivo* conditions are often affected by interactions with secondary components such as lipids [26]. Ionic surfactants are structurally similar to lipids constituting the biological membranes and have been reported to induce amyloid-like fibril formation of various proteins through hydrophobic and electrostatic interactions [27]. Sodium dodecyl sulphate (SDS) is an anionic surfactant which exhibits fibrillation inducing effects at low (<150 μM) concentrations [28]. Fibril inhibitory or modulatory innovations using plant bioactives in SDS induced biomimetic conditions are but few [29].

This work has been designed to investigate the effects of flavonoligan SB on SDS induced HSA fibrillation after a preliminary understanding of protein-SB interactions. Although there are numerous proteins (such as insulin, α-synuclein, lysozyme, β2 microglobulin) that produce amyloid-like fibrils under *in vitro* conditions, HSA is one widely studied model protein used to understand the molecular effects of various inhibitors or disruptors of fibril formations [30,31]. Besides possessing amyloidogenic characteristics, HSA attracts considerable interests in the area of drug delivery due to its ability to bind with a variety of molecules [32]. HSA is a typical α-helical (>60%), single chained protein containing 585 amino acids arranged exquisitely in three homologous domains [33]. It has been long established that the systematic aggregation of albumin occurs through partial misfolding of its native structure and this process can replicated *in vitro* through specific conditions such as high temperature, metal ions interactions, treatment with denaturing chemicals, and lowering of pH [34]. The aggregates often feature cross-β sheets which are the target sites for different amyloid binding dye molecules, such as thioflavin T and Congo red [35,36]. Incubation of HSA protein with SDS molecules was considered to be an excellent model to understand the generic mechanism through which oligomeric intermediates interact with cell membranes, and disrupt the membrane integrity.

2. Experimental

2.1. Materials

SB and lyophilised HSA were purchased from Sigma Aldrich, US. Thioflavin T (ThT) dye used for fibrillation experiments was purchased from TCI Chemicals, Japan, while congo red (CR) dye and sodium dodecyl sulphate (SDS) were obtained from Loba Chemie, India. Milli-Q water from laboratory purification system was used for preparation of all solutions and buffer.

2.2. Molecular docking

The molecular structures of SB and SDS were obtained from the PubChem database [37], and HSA crystal protein structure PDB ID: 2BXP was retrieved from Protein Data Bank (PDB) [38]. To perform the molecular docking, both the structures of ligands: SB, SDS and protein: HSA were prepared using the 'LigPrep' and 'Protein Preparation Wizard' modules of Schrödinger suite (Schrödinger, LLC, New York, NY. 2017) [39], respectively. During the ligand structure framing, a maximum of 32 stereoisomers were generated by retaining their optical properties, and three-dimensional (3D) low-energy isomers obtained for SDS and SB. On the other hand, while preparation of HSA structure, certain steps were followed such as removal of attached ligand and water molecules, repairing of side and backbone chain atoms, refinement of disordered loops, and assignment of appropriate bond orders. After optimization of hydrogen bond assignment to the protein structure, a restrained minimization process was performed using OPLS2005 force field, in order to achieve the minimum energy conformation for the HSA. Thereafter, a grid was prepared using the 'Receptor Grid Generation' tool of Schrödinger suite in Maestro user interface [39]. The co-crystal ligand information was used for grid file preparation and the centroid dimension was set to 25 Å. At first, rigid receptor Glide-XP docking was executed where HSA protein considered as rigid [40]. After successful execution of XP docking, the best docked pose was analyzed. Then Induced Fit Docking (IFD) protocol was implemented where flexibility was crucially considered for both ligand and receptor [41]. Initially, each ligand was docked into the rigid receptor with the default setting and a maximum of 20 poses per ligand were obtained. In the following step, all the receptor-ligand complexes were sampled and refined. Then, re-docking of the ligand was performed for the complexes found within the 30 kcal mol^{-1} of the lowest-energy structure. In this stage, the IFD scores were generated (i.e. GlideScore + 5% Prime Energy), as the ligand was re-docked into refined low energy induced fit structure and IFD scores were ranked for convenience of analysis. All molecular interactions were observed using 2D interaction diagram tool of Schrödinger suite in Maestro user interface [39].

2.3. HSA solution preparation and SDS-induced fibril formations

Protein stock solution was constituted by dissolving HSA in buffer solution (10 mM PBS, pH 7.4), and the concentration was spectrophotometrically fixed to 100 μM using a molar extinction co-efficient of 35,219 M^{-1} cm^{-1} at 280 nm [42].

To understand the effects of SB on HSA fibrillation in presence of SDS, HSA (10 μM) fibril formation was allowed at different concentrations of SB (0, 10, 20, 30, 40, 50 μM). HSA solutions containing 80 μM SDS were incubated at 37 ± 2 °C for 48 h and aliquots of samples were diluted accordingly for subsequent analysis.

2.4. Turbidity measurement

Turbidity of incubated samples were recorded on a double-beam UV–visible spectrophotometer (UV-1800, Shimadzu Corp., Japan) using quartz cuvettes of 1 cm path length. Absorbance of protein samples incubated with and without SB were recorded at 350 nm.

2.5. Congo red (CR) dye binding

200 μL of stock CR dye (40 μM) was mixed with 800 μL of treated HSA solutions to produce a final dye and protein molar ratio of 1:1. Dyed solutions were incubated in dark for 30 min and absorption spectra were obtained using a UV–visible spectrophotometer [43]. Amyloid formations were detected from bathochromic shifts of CR absorption peak in the range of 350–600 nm.

2.6. Thioflavin T (ThT) fluorescence spectroscopy

HSA samples were incubated with ThT dye solution in the dark for 10 min, so that the final ratio of dye and protein were 5:1 [44]. The fluorescence intensities were then recorded on a spectrofluorimeter (PerkinElmer LS-5, PerkinElmer Inc., US), having excitation and emission wavelengths fixed at 450 and 480 nm. The excitation and emission slit widths were set to 2 nm. Fresh HSA, SDS and SB were also checked to confirm non-responsiveness to ThT fluorescence.

2.7. Circular dichroism (CD)

Far UV-CD spectra between 190 and 250 nm were obtained on a CD spectropolarimeter (Jasco J-815, Jasco Corp., Japan) set with a scan rate of 100 nm min^{-1} and bandwidth of 1 nm. Diluted samples were taken in a 1 mm cell and all experiments were performed at 25 ± 2 °C. Each spectrum was baseline corrected and ellipticity was derived from an average of three scans acquired.

2.8. Transmission electron microscopy (TEM)

Structures of HSA fibrils were examined through transmission electron microscopy. 15 μL of sample was placed on a carbon coated copper

grid (Ted Pella, US) and negatively stained with uranyl acetate (2%, w/v) solution. Excess of the stain was removed and grids were left to air dry. Micrographs were captured on an electron microscope (JEOL JEM 2100 HR, Japan) operated at 120 kV.

2.9. Statistical analysis

All the experiments were done in triplicates and data have been represented as mean ± standard deviations (S.D.).

3. Results and discussion

3.1. SB-HSA interaction study

The molecular binding interaction and binding affinities for both the compounds SDS and SB were investigated using *in silico* techniques. For each compound, the best dock pose selection was made based on lowest docking score. Evaluation of Glide XP docking score revealed that SB showed much greater and better docking score (i.e. −10.54 kcal mol^{-1}), than the compound SDS which exhibited relatively less Glide XP docking score i.e. −6.07 kcal mol^{-1}. The analysis of IFD score also corroborated with the obtained XP docking result, as IFD scores were found to be −1256.76 and −967.27 kcal mol^{-1} for compound SB and SDS, respectively. In general, higher negative docking score indicates better binding affinity of any ligand towards the protein target. The binding mode of SB with HSA was represented by several numbers of hydrogen bonds and one pi-cation interaction. Docking obtained 2D and 3D binding orientations of SB have been displayed in Fig. 1A, respectively. Detailed observation revealed that amino acid residues GLU 153, LYS 199, ARG 257, SER 287 and GLU 292 extended for hydrogen bond interactions formation. Among the above mentioned residues, basic amino acid ARG 257 of HSA participated to form pi-cation interaction with SB. Mostly, the hydroxyl groups of SB act as hydrogen bond acceptors for formation of hydrogen bond with HSA. All hydrogen bond interactions were observed to occur within a distance of 1.77–2.19 Å. Apart from hydrogen bond interactions, several hydrophobic residues such as LEU 219, PHE 223, LEU 234, ALA 258, LEU 260, ALA 261, ILE 264, ILE 290 and ALA 291 were also found in close proximity and might be accounted for exposing hydrophobic contacts with SB. Bond lengths between SB and HSA were further calculated and were found to be similar to the data recorded in previous works [45]. On the other hand, binding mode and molecular interaction of SDS with HSA depicted in Fig. 1B, which demonstrated only one hydrogen bond interaction with residue TRP 214. In our previous work, importance of this TRP 214 residue of HSA protein established with a diterpenoid compound andrographolide through hydrophobic interactions [46]. Earlier, molecular docking studies of small molecules with HSA have demonstrated involvement of similar types of residues and were majorly mediated by hydrogen bonds and

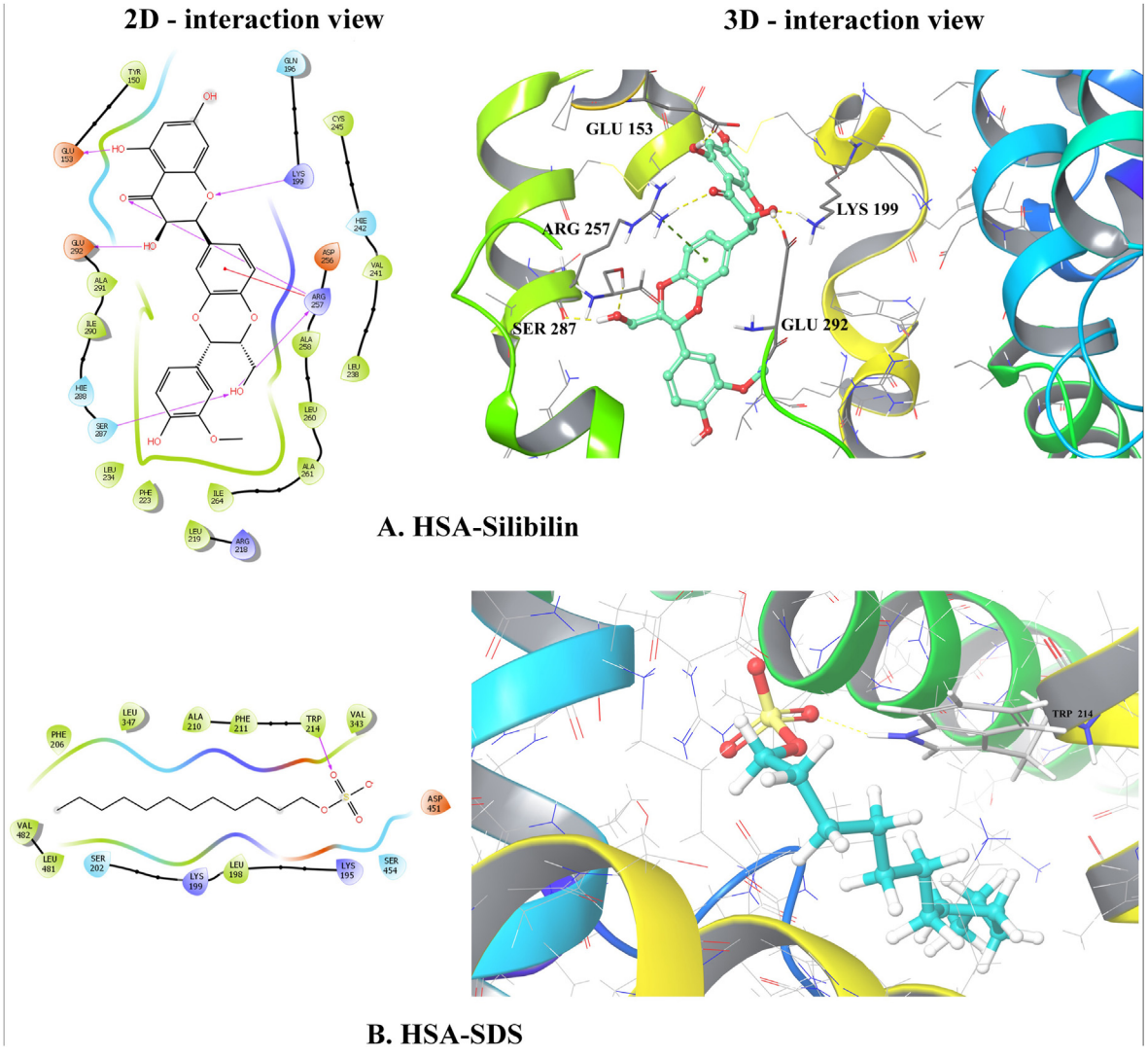

Fig. 1. 2D and 3D view of crystal structure of human serum albumin (PDB ID: 2BXP) docked to (A) SB and (B) SDS.

hydrophobic interactions [47–49]. Overall, findings of molecular modeling study demonstrated that flavonolignan SB has higher capacity to bind with HSA, and can be possibly strip the bound SDS molecules from protein surface [29]. This observation is supported by greater docking score obtained for SB in both the docking method used to predict the binding mode and affinity analysis. SB can thereby be explored as one inhibitor of HSA fibril formation in presence of SDS.

3.2. Effect of silibinin on HSA fibrillation

Low concentration SDS induced self-aggregation of serum albumin [28] was observed throughout and final absorbance at 350 nm recorded after 48 h were presented in Fig. 2. Increased population of protein oligomers in solution cause cloudiness and rise in intensity of light scattering [50]. Turbidity of HSA in absence of SDS appeared minimum, which indicated presence of soluble protein structures. Addition of 80 μM SDS resulted in cloudy appearance of the protein solution along with an immense increase in absorbance. This was probably due to generation of protein aggregates. However, a fall in absorbance were observed when HSA was incubated with increasing concentrations (10–50 μM) of SB. The maximum effect was recorded at 50 μM concentration of SB. Decrease in turbidity could be attributed to reduction in number of aggregates upon SB co-incubation [51]. Turbidity of incubated solutions thus provided the preliminary evidences of the protein-SB molecular interactions in presence of SDS and their effects on HSA fibrillation were outlined.

Systemic association of amyloidogenic proteins are often characterized by rich β-sheet structures [52]. CR is one anionic dye which exhibits maximum absorbance at 490 nm in PBS pH 7.4 medium [53]. The dye molecules interact with ordered aggregates containing cross β-sheet rich conformations to produce a characteristic red shift [54]. SDS treated HSA samples had bound to the dye and exhibited a significant red shift of the spectra to 511 nm, much in contrast to native HSA spectrum (Fig. 3). This indicated the growth of β-sheet rich structures in presence of SDS upon incubation for 48 h. Presence of SB in protein solution, however, restricted the shift of CR absorption maxima within 499 nm. This was likely due to inhibition of HSA fibrillation.

ThT is an amyloid specific biomarker which produces an unique fluorescence quantum yield upon binding to the β-sheets of amyloids [55]. It is routinely used in quantitative investigation of amyloid fibrils, and was applied in this work to complement the turbidity and congo red assays [56]. Native HSA sample did not exhibit significant ThT response at 480 nm due to its un-aggregated state (Fig. 4a). Addition of SDS solution (80 μM) triggered a distinct increase in ThT response, signifying a high density of HSA fibrillar species. At 80 μM concentration, SDS molecules associate with HSA leading to displacement of water from the immediate vicinity [57]. The association is mainly due to electrostatic charge interactions, though hydrophobic interactions also co-exist [58]. These events are reported as spontaneous and cause fibrillation of HSA through continuous accretion [59]. Co-incubation with ascending concentrations of SB, however, lowered the ThT intensity with the maximum effect observed for 50 μM SB. A mild decrease of 8% in ThT intensity was recorded with 10 μM SB co-incubation, whereas the ThT response for SDS treated protein samples decreased by 36% in presence of 50 μM of SB (Fig. 4b).

3.3. Effect of silibinin on HSA secondary structure

Changes in the secondary structure of HSA upon addition of SDS and SB were further investigated through far UV CD spectroscopy (Fig. 5). Native HSA at 25 ± 2 °C exhibits two negative peaks at 208 nm and 222 nm, due to its prevailing α-helical or random coil conformation [60,61]. Loss of the dual minima in presence of SDS indicated a shift from native secondary structure. SDS treatment also produced a negative peak at 216 nm due to presence of cross β-sheet contents [62]. This is the distinctive feature of all amyloid fibrils. Previous reports showed that SDS in low concentrations triggered that transformation of α-helical to β-sheets elements in lysozyme [29], HSA [28] and α-synuclein [59]. Presence of low concentrations of SB (10–20 μM) did not have significant effect on the spectra of SDS treated HSA. Increase in SB concentration (30–50 μM) in solution however weakened the signal at 216 nm and caused partial restoration of negative ellipticities at 208 and 222 nm. CD experiments suggested that while SDS treatment caused disruption in α-helical form, SB was able to limit the formation of β-sheets and prevented complete loss of native albumin structure.

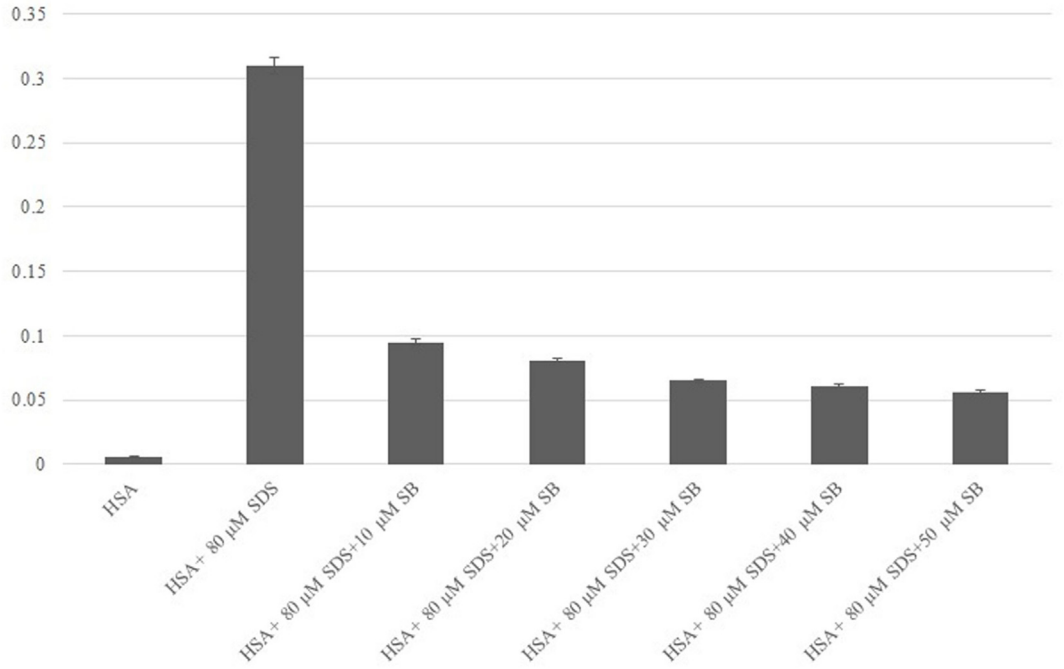

Fig. 2. Turbidity of HSA at 350 nm in presence and absence of SDS and SB. Absorbance are expressed as mean ± S.D. (n = 3).

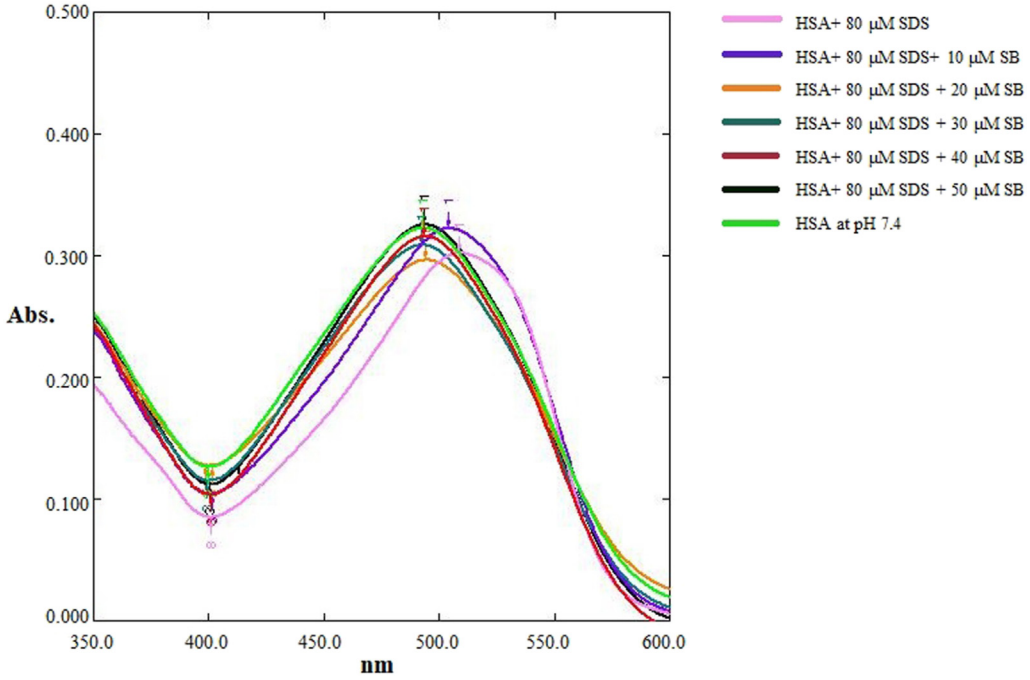

Fig. 3. CR absorption spectra of HSA samples incubated in presence and absence of SB and SDS.

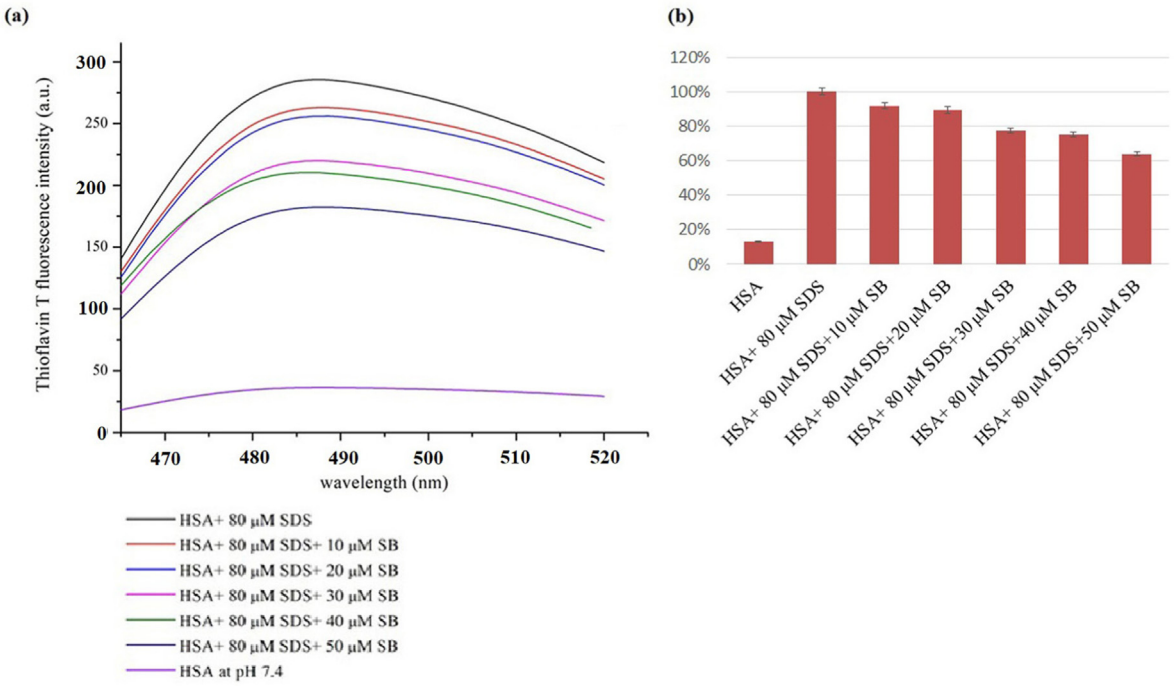

Fig. 4. (a) ThT fluorescence spectra of HSA in presence and absence of SDS and SB (b) Fluorescence emission intensity at 480 nm in presence and absence of SDS and SB.

3.4. Morphological evaluations

Morphological evidences of SDS induced HSA fibrillation and effects of bioactive SB on fibril formations were recorded through electron microscopy. TEM is a powerful tool often used to study the morphology and abundance of different amyloid fibrils [63–66]. Typical amyloid fibrils are known to possess diameters of 8–12 nm, and may be several micrometers long [67]. High resolution micrographs showed that HSA upon incubation with SDS for 48 h resulted in formation of profuse branched structures (Fig. 6a), which are the characteristics of mature amyloid fibrils [34,68]. Samples incubated with increasing concentrations of SB revealed sparing populations of fibrils (Fig. 6b–e). The structures appeared less fibrillar and not well-defined at higher concentrations of SB (Fig. 6f). These observations corroborated the spectroscopic data and confirmed a dose dependent protein-fibrillation inhibitory effect of SB.

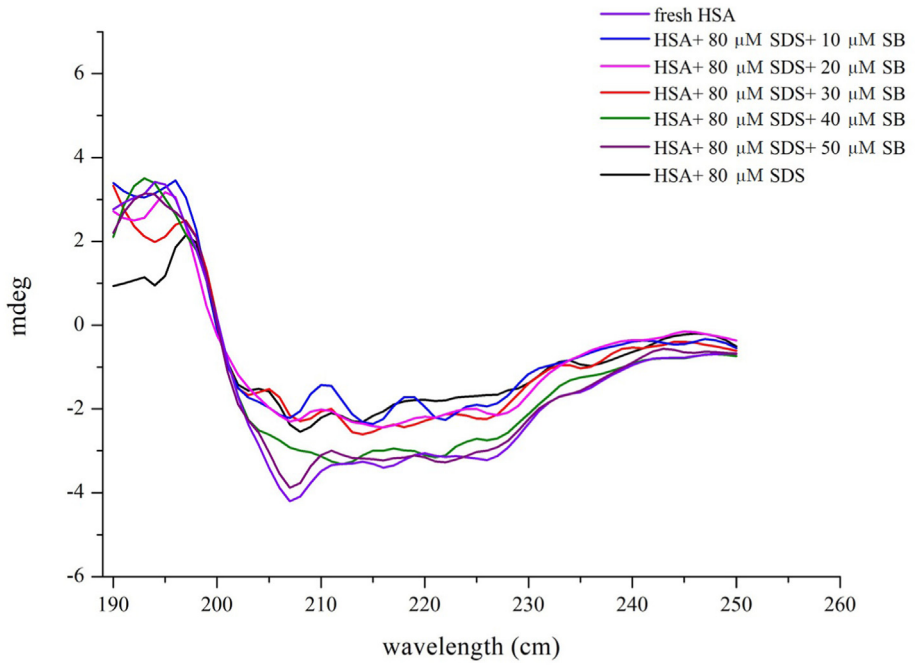

Fig. 5. CD spectra of HSA in absence and presence of SDS and SB.

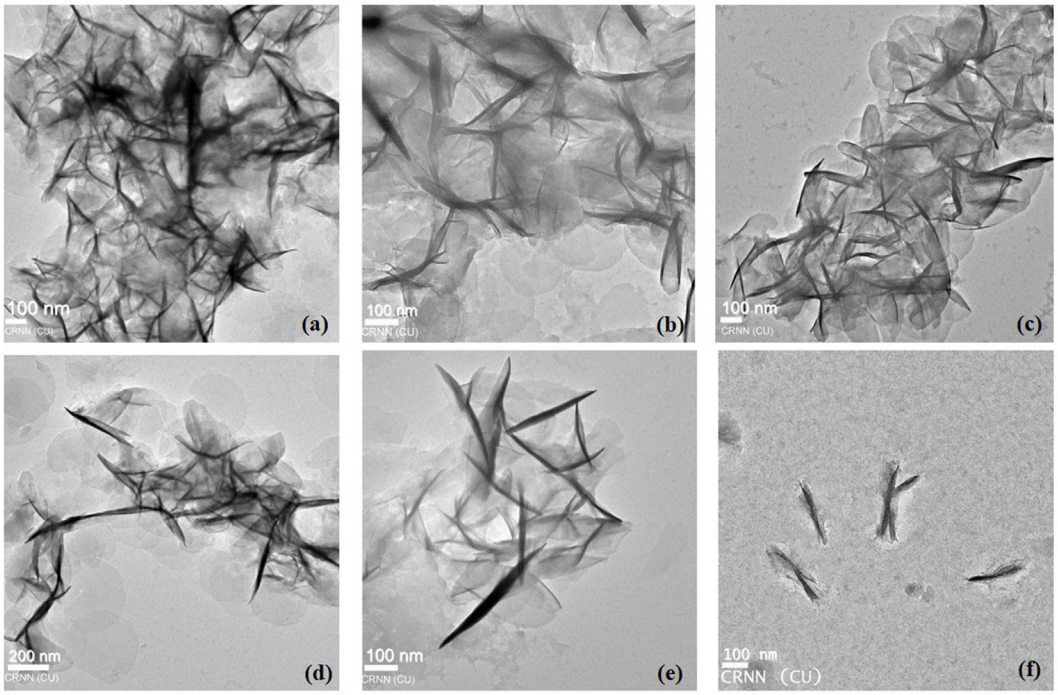

Fig. 6. Electron micrographs of SDS treated HSA incubated in (a) absence and (b–f) presence of different concentrations (10–50 μM) of SB. Scale 100 nm.

4. Conclusion

Protein fibrillation and amyloidogenesis are unscrupulous physiological events and often lead to a number of degenerative conditions in humans. In the present work, SDS induced protein fibril formation was studied through a variety of biophysical, microscopic techniques and *in silico* docking studies. Turbidity assay demonstrated that aggregation propensity of HSA is maximum at 48 h in presence of 0.8 mM SDS. SB, a flavonolignan was investigated as one molecular scaffold for inhibition of HSA protein fibrillation. SB expressed an inhibitory capacity against SDS induced HSA fibrillation. That effect was due to multiple hydrogen bonds and hydrophobic interactions in molecular interfaces. Molecular docking experiments also revealed that the SB has a much higher binding affinity towards albumin, and can possibly strip the SDS molecules from the protein binding sites. Protein secondary structure evaluations and morphology studies confirmed concentration dependent inhibitory effects of SB. Electron micrographs showed less fibril-like networks when HSA was incubated with SB at 1:5 molar ratio, thus confirming their fibril recessive effects. A combination of different spectrometric studies revealed that 36% inhibition of HSA fibril formation appeared at a HSA:

SB molar ratio of 1:5. HSA structural stabilization through preferential binding of SB was the guiding factor for restricting the formation of protein fibrils in presence of SDS. SB may therefore be considered as an appropriate molecular scaffold for inhibition of fibril formation and enhance our understanding on therapeutic interventions in amyloid related degenerative diseases.

CRediT authorship contribution statement

Aalok Basu: Methodology, Investigation, Formal analysis, Validation, Writing – original draft. **Shovonlal Bhowmick:** Investigation, Writing – original draft, Software. **Arup Mukherjee:** Conceptualization, Supervision, Project administration.

Declaration of competing interest

Authors would like to declare that there is no conflict of interest in publication of this article.

Acknowledgements

Authors would acknowledge financial aids received from TEQIP project in University of Calcutta.

References

[1] Rabbani G, Ahmad E, Zaidi N, Khan RH. pH-dependent conformational transitions in conalbumin (ovotransferrin), a metalloproteinase from hen egg white. Cell Biochem. Biophys. 2011;61:551–60. https://doi.org/10.1007/s12013-011-9237-x.

[2] Rabbani G, Ahmad E, Zaidi N, Fatima S, Khan RH. pH-induced molten globule state of rhizopus niveus lipase is more resistant against thermal and chemical denaturation than its native state. Cell Biochem. Biophys. 2012;62:487–99. https://doi.org/10.1007/s12013-011-9335-9.

[3] Morel B, Conejero-Lara F. Early mechanisms of amyloid fibril nucleation in model and disease-related proteins. Biochim. Biophys. Acta Protein Proteonomics 2019; 1867:140264. https://doi.org/10.1016/j.bbapap.2019.140264.

[4] Rabbani G, Kaur J, Ahmad E, Khan RH, Jain SK. Structural characteristics of thermostable immunogenic outer membrane protein from Salmonella enterica serovar Typhi. Appl. Microbiol. Biotechnol. 2014;98:2533–43. https://doi.org/10.1007/s00253-013-5123-3.

[5] Rabbani G, Ahmad E, Khan MV, Ashraf MT, Bhat R, Khan RH. Impact of structural stability of cold adapted Candida Antarctica lipase B (CaLB): in relation to pH, chemical and thermal denaturation. RSC Adv. 2015;5:20115–31. https://doi.org/10.1039/C4RA17093H.

[6] Meesaragandla B, Karanth S, Janke U, Delcea M. Biopolymer-coated gold nanoparticles inhibit human insulin amyloid fibrillation. Sci. Rep. 2020;10:7862. https://doi.org/10.1038/s41598-020-64010-7.

[7] Chiti & Dobson. Amyloid formation, protein homeostasis, and human disease: a summary of progress over the last decade. Annu. Rev. Biochem. 2017;86:1–42. https://doi.org/10.1146/annurev-biochem-061516-045115.

[8] Sen P, Ahmad B, Rabbani G, Khan RH. 2,2,2-Trifluroethanol induces simultaneous increase in α-helicity and aggregation in alkaline unfolded state of bovine serum albumin. Int. J. Biol. Macromol. 2010;46:250–4. https://doi.org/10.1016/j.ijbiomac.2009.12.013.

[9] Mandal S, Panja P, Debnath K, Jana NR, Jana NR. Small-molecule-functionalized hyperbranched polyglycerol dendrimers for inhibiting protein aggregation. Biomacromolecules 2020;21:3270–8. https://doi.org/10.1021/acs.biomac.0c00713.

[10] Henríquez G, Gomez A, Guerrero E, Narayan M. Potential role of natural polyphenols against protein aggregation toxicity: in vitro, in vivo, and clinical studies. ACS Chem. Neurosci. 2020;11:2915–34. https://doi.org/10.1021/acschemneuro.0c00381.

[11] Hao S, Li X, Han A, Yang Y, Luo X, Fang G, Wang H, Liu J, Wang S. Hydroxycinnamic acid from corncob and its structural analogues inhibit Aβ40 fibrillation and attenuate aβ40-induced cytotoxicity. J. Agric. Food Chem. 2020;68: 8788–96. https://doi.org/10.1021/acs.jafc.0c01841.

[12] Siegel AB, Stebbing J. Milk thistle: early seeds of potential. Lancet Oncol. 2013;14: 929–30. https://doi.org/10.1016/S1470-2045(13)70414-5.

[13] Saller R, Meier R, Brignoli R. The use of silymarin in the treatment of liver diseases. Drugs 2001;61:2035–63. https://doi.org/10.2165/00003495-200161140-00003.

[14] Delmas D. Silymarin and derivatives: from biosynthesis to health benefits. Mol 2020;25. https://doi.org/10.3390/molecules25102415.

[15] Lee JI, Narayan M, Barrett JS. Analysis and comparison of active constituents in commercial standardized silymarin extracts by liquid chromatography–electrospray ionization mass spectrometry. J. Chromatogr. B. 2007;845:95–103. https://doi.org/10.1016/j.jchromb.2006.07.063.

[16] Federico A, Dallio M, Masarone M, Gravina AG, Di Sarno R, Tuccillo C, Cossiga V, Lama S, Stiuso P, Morisco F, Persico M, Loguercio C. Evaluation of the effect derived from silybin with vitamin D and vitamin E administration on clinical, metabolic, endothelial dysfunction, oxidative stress parameters, and serological worsening markers in nonalcoholic fatty liver disease patients. Oxid. Med. Cell. Longev. 2019; 2019:8742075. https://doi.org/10.1155/2019/8742075.

[17] Tao L, Qu X, Zhang Y, Song Y, Zhang S. Prophylactic therapy of silymarin (milk thistle) on antituberculosis drug-induced liver injury: a meta-analysis of randomized controlled trials. Chin. J. Gastroenterol. Hepatol. 2019;2019:3192351. https://doi.org/10.1155/2019/3192351.

[18] Trouillas P, Marsal P, Svobodová A, Vostálová J, Gažák R, Hrbáč J, Sedmera P, Křen V, Lazzaroni R, Duroux J-L, Walterová D. Mechanism of the antioxidant action of silybin and 2,3-dehydrosilybin flavonolignans: a joint experimental and theoretical study. J. Phys. Chem. A. 2008;112:1054–63. https://doi.org/10.1021/jp075814h.

[19] Trappoliere M, Caligiuri A, Schmid M, Bertolani C, Failli P, Vizzutti F, Novo E, di Manzano C, Marra F, Loguercio C, Pinzani M. Silybin, a component of sylimarin, exerts anti-inflammatory and anti-fibrogenic effects on human hepatic stellate cells. J. Hepatol. 2009;50:1102–11. https://doi.org/10.1016/j.jhep.2009.02.023.

[20] Das S, Roy P, Pal R, Auddy RG, Chakraborti AS, Mukherjee A. Engineered silybin nanoparticles educe efficient control in experimental diabetes. PLoS One 2014;9. https://doi.org/10.1371/journal.pone.0101818. e101818–e101818.

[21] Liu P, Cui L, Liu B, Liu W, Hayashi T, Mizuno K, Hattori S, Ushiki-Kaku Y, Onodera S, Ikejima T. Silibinin ameliorates STZ-induced impairment of memory and learning by up- regulating insulin signaling pathway and attenuating apoptosis. Physiol. Behav. 2020;213:112689. https://doi.org/10.1016/j.physbeh.2019.112689.

[22] Cheng B, Gong H, Li X, Sun Y, Zhang X, Chen H, Liu X, Zheng L, Huang K. Silibinin inhibits the toxic aggregation of human islet amyloid polypeptide. Biochem. Biophys. Res. Commun. 2012;419:495–9. https://doi.org/10.1016/j.bbrc.2012.02.042.

[23] Yin F, Liu J, Ji X, Wang Y, Zidichouski J, Zhang J. Silibinin: a novel inhibitor of Aβ aggregation. Neurochem. Int. 2011;58:399–403. https://doi.org/10.1016/j.neuint.2010.12.017.

[24] Katebi B, Mahdavimehr M, Meratan AA, Ghasemi A, Nemat-Gorgani M. Protective effects of silibinin on insulin amyloid fibrillation, cytotoxicity and mitochondrial membrane damage. Arch. Biochem. Biophys. 2018;659:22–32. https://doi.org/10.1016/j.abb.2018.09.024.

[25] Rabbani G, Khan MJ, Ahmad A, Maskat MY, Khan RH. Effect of copper oxide nanoparticles on the conformation and activity of β-galactosidase. Colloids Surf. B Biointerfaces 2014;123:96–105. https://doi.org/10.1016/j.colsurfb.2014.08.035.

[26] Kollmer M, Meinhardt K, Haupt C, Liberta F, Wulff M, Linder J, Handl L, Heinrich L, Loos C, Schmidt M, Syrovets T, Simmet T, Westermark P, Westermark GT, Horn U, Schmidt V, Walther P, Fändrich M. Electron tomography reveals the fibril structure and lipid interactions in amyloid deposits. Proc. Natl. Acad. Sci. 2016;113:5604–9. https://doi.org/10.1073/pnas.1523496113.

[27] Ismael MA, Khan JM, Malik A, Alsenaidy MA, Hidayathulla S, Khan RH, Sen P, Irfan M, Alsenaidy AM. Unraveling the molecular mechanism of the effects of sodium dodecyl sulfate, salts, and sugars on amyloid fibril formation in camel IgG. Colloids Surf. B Biointerfaces 2018;170:430–7. https://doi.org/10.1016/j.colsurfb.2018.06.035.

[28] Movaghati S, Moosavi-Movahedi AA, Khodagholi F, Digaleh H, Kachooei E, Sheibani N. Sodium dodecyl sulphate modulates the fibrillation of human serum albumin in a dose-dependent manner and impacts the PC12 cells retraction. Colloids Surf. B Biointerfaces 2014;122:341–9. https://doi.org/10.1016/j.colsurfb.2014.07.002.

[29] Khan JM, Malik A, Rehman T, AlAjmi MF, Alamery SF, Alghamdi OHA, Khan RH, Odeibat HAM, Fatima S. Alpha-cyclodextrin turns SDS-induced amyloid fibril into native-like structure. J. Mol. Liq. 2019;289:111090. https://doi.org/10.1016/j.molliq.2019.111090.

[30] Juárez J, López SG, Cambón A, Taboada P, Mosquera V. Influence of electrostatic interactions on the fibrillation process of human serum albumin. J. Phys. Chem. B 2009;113:10521–9. https://doi.org/10.1021/jp902224d.

[31] Bag S, Mitra R, DasGupta S, Dasgupta S. Inhibition of human serum albumin fibrillation by two-dimensional nanoparticles. J. Phys. Chem. B 2017;121:5474–82. https://doi.org/10.1021/acs.jpcb.7b01289.

[32] Rabbani G, Ahn SN. Structure, enzymatic activities, glycation and therapeutic potential of human serum albumin: a natural cargo. Int. J. Biol. Macromol. 2019; 123:979–90. https://doi.org/10.1016/j.ijbiomac.2018.11.053.

[33] Xu L, Hu YX, Li YC, Zhang L, Ai HX, Liu HS, Liu YF, Sang YL. Study on the interaction of tussilagone with human serum albumin (HSA) by spectroscopic and molecular docking techniques. J. Mol. Struct. 2017;1149:645–54. https://doi.org/10.1016/j.molstruc.2017.08.039.

[34] Taboada P, Barbosa S, Castro E, Mosquera V. Amyloid fibril formation and other aggregate species formed by human serum albumin association. J. Phys. Chem. B 2006;110:20733–6. https://doi.org/10.1021/jp064861r.

[35] Ghosh R, Kishore N. Physicochemical insights into the role of drug functionality in fibrillation inhibition of bovine serum albumin. J. Phys. Chem. B 2020;124: 8989–9008. https://doi.org/10.1021/acs.jpcb.0c06167.

[36] Espargaró A, Llabrés S, Saupe SJ, Curutchet C, Luque FJ, Sabaté R. On the binding of Congo red to amyloid fibrils. Angew. Chem. Int. Ed. 2020;59:8104–7. https://doi.org/10.1002/anie.201916630.

[37] Kim S, Thiessen PA, Bolton EE, Chen J, Fu G, Gindulyte A, Han L, He J, He S, Shoemaker BA. PubChem substance and compound databases. Nucleic Acids Res. 2016;44:D1202–13.

[38] Berman HM, Westbrook J, Feng Z, Gilliland G, Bhat TN, Weissig H, Shindyalov IN, Bourne PE. The protein Data Bank. Nucleic Acids Res. 2000;28:235–42. https://doi.org/10.1093/nar/28.1.235.

[39] Maestro S. New York, NY: LLC; 2017.
[40] Friesner RA, Murphy RB, Repasky MP, Frye LL, Greenwood JR, Halgren TA, Sanschagrin PC, Mainz DT. Extra precision Glide: docking and scoring incorporating a model of hydrophobic enclosure for Protein−Ligand complexes. J. Med. Chem. 2006;49:6177–96. https://doi.org/10.1021/jm051256o.
[41] Sherman W, Beard HS, Farid R. Use of an induced fit receptor structure in virtual screening. Chem. Biol. Drug Des. 2006;67:83–4. https://doi.org/10.1111/j.1747-0285.2005.00327.x.
[42] Rabbani G, Lee EJ, Ahmad K, Baig MH, Choi I. Binding of tolperisone hydrochloride with human serum albumin: effects on the conformation, thermodynamics, and activity of HSA. Mol. Pharm. 2018;15:1445–56. https://doi.org/10.1021/acs.molpharmaceut.7b00976.
[43] Furkan M, Sidddiqi MK, Khan AN, Khan RH. An antibiotic (sulfamethoxazole) stabilizes polypeptide (human serum albumin) even under extreme condition (elevated temperature). Int. J. Biol. Macromol. 2019;135:337–43. https://doi.org/10.1016/j.ijbiomac.2019.05.152.
[44] Sen S, Konar S, Das B, Pathak A, Dhara S, Dasgupta S, DasGupta S. Inhibition of fibrillation of human serum albumin through interaction with chitosan-based biocompatible silver nanoparticles. RSC Adv. 2016;6:43104–15. https://doi.org/10.1039/C6RA05129D.
[45] Maiti TK, Ghosh KS, Samanta A, Dasgupta S. The interaction of silibinin with human serum albumin: a spectroscopic investigation. J. Photochem. Photobiol. A Chem. 2008;194:297–307. https://doi.org/10.1016/j.jphotochem.2007.08.028.
[46] Basu A, Bhayye S, Kundu S, Das A, Mukherjee A. Andrographolide inhibits human serum albumin fibril formations through site-specific molecular interactions. RSC Adv. 2018;8:30717–24. https://doi.org/10.1039/C8RA04637A.
[47] Abdullah SMS, Fatma S, Rabbani G, Ashraf JM. A spectroscopic and molecular docking approach on the binding of tinzaparin sodium with human serum albumin. J. Mol. Struct. 2017;1127:283–8. https://doi.org/10.1016/j.molstruc.2016.07.108.
[48] Varshney A, Rehan M, Subbarao N, Rabbani G, Khan RH. Elimination of endogenous toxin, creatinine from blood plasma depends on albumin conformation: site specific uremic toxicity & impaired drug binding. PLoS One 2011;6:e17230. https://doi.org/10.1371/journal.pone.0017230.
[49] Ahmad E, Rabbani G, Zaidi N, Singh S, Rehan M, Khan MM, Rahman SK, Quadri Z, Shadab M, Ashraf MT, Subbarao N, Bhat R, Khan RH. Stereo-selectivity of human serum albumin to enantiomeric and isoelectronic pollutants dissected by spectroscopy, calorimetry and bioinformatics. PLoS One 2011;6:e26186. https://doi.org/10.1371/journal.pone.0026186.
[50] Fazili NA, Naeem A. Anti-fibrillation potency of caffeic acid against an antidepressant induced fibrillogenesis of human α-synuclein: implications for Parkinson's disease. Biochimie 2015;108:178–85. https://doi.org/10.1016/j.biochi.2014.11.011.
[51] Chaturvedi SK, Zaidi N, Alam P, Khan JM, Qadeer A, Siddique IA, Asmat S, Zaidi Y, Khan RH. Unraveling comparative anti-amyloidogenic behavior of pyrazinamide and D-cycloserine: a mechanistic biophysical insight. PLoS One 2015;10:e0136528. https://doi.org/10.1371/journal.pone.0136528.
[52] Chaturvedi SK, Siddiqi MK, Alam P, Khan RH. Protein misfolding and aggregation: mechanism, factors and detection. Process Biochem. 2016;51:1183–92. https://doi.org/10.1016/j.procbio.2016.05.015.
[53] Khan MV, Ishtikhar M, Rabbani G, Zaman M, Abdelhameed AS, Khan RH. Polyols (Glycerol and Ethylene glycol) mediated amorphous aggregate inhibition and secondary structure restoration of metalloproteinase-conalbumin (ovotransferrin). Int. J. Biol. Macromol. 2017;94:290–300. https://doi.org/10.1016/j.ijbiomac.2016.10.023.
[54] Siddiqi MK, Alam P, Chaturvedi SK, Nusrat S, Shahein YE, Khan RH. Attenuation of amyloid fibrillation in presence of Warfarin: a biophysical investigation. Int. J. Biol. Macromol. 2017;95:713–8. https://doi.org/10.1016/j.ijbiomac.2016.11.110.
[55] Alam P, Siddiqi MK, Malik S, Chaturvedi SK, Uddin M, Khan RH. Elucidating the inhibitory potential of Vitamin A against fibrillation and amyloid associated cytotoxicity. Int. J. Biol. Macromol. 2019;129:333–8. https://doi.org/10.1016/j.ijbiomac.2019.01.134.
[56] Khan MV, Rabbani G, Ishtikhar M, Khan S, Saini G, Khan RH. Non-fluorinated cosolvents: a potent amorphous aggregate inducer of metalloproteinase-conalbumin (ovotransferrin). Int. J. Biol. Macromol. 2015;78:417–28. https://doi.org/10.1016/j.ijbiomac.2015.04.021.
[57] Mukherjee S, Sen P, Halder A, Sen S, Dutta P, Bhattacharyya K. Solvation dynamics in a protein–surfactant aggregate. TNS in HSA–SDS. Chem. Phys. Lett. 2003;379:471–8. https://doi.org/10.1016/j.cplett.2003.08.085.
[58] Gelamo EL, Tabak M. Spectroscopic studies on the interaction of bovine (BSA) and human (HSA) serum albumins with ionic surfactants. Spectrochim. Acta Part A Mol. Biomol. Spectrosc. 2000;56:2255–71. https://doi.org/10.1016/S1386-1425(00)00313-9.
[59] Giehm L, Oliveira CLP, Christiansen G, Pedersen JS, Otzen DE. SDS-induced fibrillation of α-synuclein: an alternative fibrillation pathway. J. Mol. Biol. 2010;401:115–33. https://doi.org/10.1016/j.jmb.2010.05.060.
[60] Rabbani G, Baig MH, Lee EJ, Cho W-K, Ma JY, Choi I. Biophysical study on the interaction between eperisone hydrochloride and human serum albumin using spectroscopic, calorimetric, and molecular docking analyses. Mol. Pharm. 2017;14:1656–65. https://doi.org/10.1021/acs.molpharmaceut.6b01124.
[61] Rabbani G, Baig MH, Jan AT, Ju Lee E, Khan MV, Zaman M, Farouk A-E, Khan RH, Choi I. Binding of erucic acid with human serum albumin using a spectroscopic and molecular docking study. Int. J. Biol. Macromol. 2017;105:1572–80. https://doi.org/10.1016/j.ijbiomac.2017.04.051.
[62] Ajmal MR, Chandel TI, Alam P, Zaidi N, Zaman M, Nusrat S, Khan MV, Siddiqi MK, Shahein YE, Mahmoud MH, Badr G, Khan RH. Fibrillogenesis of human serum albumin in the presence of levodopa- spectroscopic, calorimetric and microscopic studies. Int. J. Biol. Macromol. 2017;94:301–8. https://doi.org/10.1016/j.ijbiomac.2016.10.025.
[63] Conway KA, Harper JD, Lansbury PT. Accelerated in vitro fibril formation by a mutant α-synuclein linked to early-onset Parkinson disease. Nat. Med. 1998;4:1318–20. https://doi.org/10.1038/3311.
[64] Thapa A, Jett SD, Chi EY. Curcumin attenuates amyloid-β aggregate toxicity and modulates amyloid-β aggregation pathway. ACS Chem. Neurosci. 2016;7:56–68. https://doi.org/10.1021/acschemneuro.5b00214.
[65] Wang JB, Wang YM, Zeng CM. Quercetin inhibits amyloid fibrillation of bovine insulin and destabilizes preformed fibrils. Biochem. Biophys. Res. Commun. 2011;415:675–9. https://doi.org/10.1016/j.bbrc.2011.10.135.
[66] Malishev R, Nandi S, Kolusheva S, Shaham-Niv S, Gazit E, Jelinek R. Bacoside-A, an anti-amyloid natural substance, inhibits membrane disruption by the amyloidogenic determinant of prion protein through accelerating fibril formation. Biochim. Biophys. Acta Biomembr. 2016;1858:2208–14. https://doi.org/10.1016/j.bbamem.2016.06.019.
[67] Khan JM, Malik A, Sen P, Ahmad A, Ahmed A, Atiya A. Deciphering the role of premicellar and micellar concentrations of sodium dodecyl benzenesulfonate surfactant in insulin fibrillation at pH 2.0. Int. J. Biol. Macromol. 2020;148:880–6. https://doi.org/10.1016/j.ijbiomac.2020.01.215.
[68] Save SN, Choudhary S. Effects of triphala and guggul aqueous extracts on inhibition of protein fibrillation and dissolution of preformed fibrils. RSC Adv. 2017;7:20460–8. https://doi.org/10.1039/C6RA28440J.